Talanta 82 (2010) 1511–1515

Contents lists available at ScienceDirect

Talanta

journal homepage: www.elsevier.com/locate/talanta

A highly soluble poly(3,4-ethylenedioxythiophene)-poly(styrene sulfonic acid)/Au nanocomposite for horseradish peroxidase immobilization and biosensing

JingJing Xu, Ru Peng, Qin Ran, Yuezhong Xian*, Yuan Tian, Litong Jin

Department of Chemistry, East China Normal University, 3663 Zhongshan (N) Road, Shanghai 200062, China

ARTICLE INFO

Article history:
Received 8 March 2010
Received in revised form 14 July 2010
Accepted 15 July 2010
Available online 23 July 2010

Keywords:
PEDOT-PSS conductive polymer
Au nanopartiles
Horseradish peroxidase
Direct electrochemistry
Hydrogen peroxide
Biosensor

ABSTRACT

A highly soluble poly(3,4-ethylenedioxythiophene)-poly(styrene sulfonic acid)/Au (PEDOT-PSS/Au) nanocomposite was prepared via one-step chemical synthesis and the matrix was characterized by UV–vis spectroscopy (UV–vis), Fourier transform infrared spectroscopy (FT-IR), scanning electron microscope (SEM) and transmission electron microscope (TEM). Due to the excellent aqueous compatibility and biocompatibility, the PEDOT/PSS-Au nanocomposite can be used as biomaterial for enzymes immobilization. In this system, redox enzyme, horseradish peroxidase (HRP) was integrated with PEDOT/PSS-Au nanocomposite and the direct electron transfer of HRP was observed. Moreover, we find that the HRP/PEDOT-PSS/Au modified electrode shows excellent electrocatalytic ability for H_2O_2 and the formal Michaelis–Menten constant (K_m^{app}) was 0.78 mmol/L. The response currents have good linear relation with the concentrations of H_2O_2 with a linear range from 2.0×10^{-7} to 3.8×10^{-4} mol/L.

1. Introduction

Poly(3,4-ethylenedioxythiophene) (PEDOT) was developed by the Bayer AG research laboratory in Germany in the late 1980s [1]. The research and development efforts of the recent years have quickly brought PEDOT to the forefront of the field of conducting polymers [2]. Due to its low oxidation potential, high conductivity, moderate band gap, relatively high transparency and excellent electrochromic properties, PEDOT has become one of the most exciting organic electronic materials and widely used in various electronic products, such as antistatic coatings for cathode ray tubes [3], organic thin film transistors [4], organic solar cells [5], electrochromic windows [6], and organic light-emitting diodes [7]. In addition, PEDOT shows inherent stability and more eco-friendly relative to polyaniline and polypyrrole due to the lack of undesired α, β- and β, β-couplings within the polymer backbone [2]. Notwithstanding the immense potential, the applications of PEDOT still remain challenge due to the disadvantage of being insoluble and infusible while the polymer is prepared via standard oxidative chemical or electrochemical polymerization. It is partly circumvented using a water-soluble polyelectrolyte, poly(styrene sulfonic acid) (PSS), as the charge-balancing dopant during polymerization to yield PEDOT/PSS, which resulting in a water-soluble matrix with good film forming properties, high conductivity, high visible light transmissivity, and excellent stability [2]. Moreover, the biocompatibility of PEDOT also has been demonstrated by some research group. PEDOT has been electrochemically deposited onto the neural probe electrode by Martin group, and the PEDOT substrates are found to support human neuroblastoma adhesion and neurite extension. In addition, the system shows the possibility to improve neural communication, and has been preliminarily examined for nerve cell [8]. Berggren group has developed an electrophoretic ion pump made of PEDOT-PSS to mediate electronic control of the ion homeostasis in neurons, which displays excellent biocompatibility for neuronal cells HCN-2 [9]. Furthermore, the biocompatibility of PEDOT has also been evaluated for neuron cultures [10], neural communication [11], nanobiointerface fabrication [12], protein adsorption and cells proliferation [13]. These findings suggest PEDOT may be a promising candidate for various bioengineering applications.

In recent years, metal nanoparticles have been the focus of much current research due to their unique physical and chemical properties as well as their enormous potential applications such as catalysts [14,15], nanoelectronic devices [16], magnetic devices [17], and chemical or biosensors [18–21]. In particular, gold nanoparticles (AuNPs) are used in a variety of applications in recent decades because of unique properties such as high biocompatibility, good conductivity, high catalytic activity, and size-dependent properties [22]. Especially, AuNPs combined with biomolecules are

* Corresponding author. Tel.: +86 21 62233954; fax: +86 21 62232627.
E-mail address: yzxian@chem.ecnu.edu.cn (Y. Xian).

0039-9140/$ – see front matter © 2010 Elsevier B.V. All rights reserved.
doi:10.1016/j.talanta.2010.07.033

widely expected to develop new detection systems for specific reactions between biomolecules [23].

Driven by the properties of PEDOT and AuNPs, we aim to combine the conducting polymers and metal nanoparticles in order to investigate the possibility of immobilization biomacromolecules and design a novel biosensing system. The nanostructured PEDOT-PSS with dispersion of AuNPs was prepared and well-dispersed AuNPs were easily obtained due to the embedding nanoparticles into the framework of conductive polymer, which enables to overcome the limitation of application AuNPs in biological systems due to nanoparticle aggregation and non-specific binding. In addition, the PEDOT-PSS/Au nanocompistes have high solubility in aqueous solution, whose colloidal solutions exhibit unsurpassed stability even for 1 year. Thus, the aqueous compatibility and biocompatibility of the nanocomposite could provide an ideal microenviroment for biomacromolecule immobilization. Moreover, the AuNPs encapsulated in PEDOT/PSS film can act as an electron relays to enhance electron exchange and realize the direct electrochemistry of redox enzymes. Herein, horseradish peroxidase (HRP), an extracellular plant enzyme, is chosen as model target and encapsulated into PEDOT-PSS/Au nanocomposites. We find that HRP in PEDOT-PSS/Au nanocomposites retains its bioactivity. Furthermore, the direct electron transfer and bioelectrocatalytic activity of HRP is observed, indicating PEDOT-PSS/Au nanocomposite is an excellent biomaterial for enzymes immobilzation and bioelectrochemical device fabrication. As far as we are aware, there is no report on immobilzation HRP in highly soluble PEDOT-PSS/Au nanocomposite and enhance the protein electrochemistry. In addition, the biocatalysis of HRP/PEDOT-PSS/Au system is applied for hydrogen peroxide biosensing.

2. Experiment

2.1. Reagents

HRP (298 U/mg, MW 44 kDa, Sigma), 3,4-ethylenedioxythiophene (EDOT) and PSS were purchased from Sigma–Aldrich. Other chemical were of analytical grade and used without further purification. Phosphate buffer solution (PBS, 0.2 mol/L) with various pH values was prepared by mixing calculated $Na_2HPO_4{\cdot}12H_2O$ and KH_2PO_4. All solutions were made up with twice-distilled water.

2.2. Synthesis of the PEDOT-PSS/Au nanocomposite

The soluble PEDOT-PSS/Au nanocomposite was prepared via one-step chemical synthesis [24]. In briefly, EDOT aqueous solution is prepared by dissolving aliquot PSS (10 mg/ml) into the water and agitating severely. After that, 36 mg EDOT is added with severe stirring. Then, an aliquot of $AuCl_3{\cdot}4H_2O$ (10 mmol/L) is slowly added to the former solution, and ensure the EDOT is superfluous to reduce the Au^{3+} to Au^0. After 12 h reaction, the PEDOT-PSS/Au nanomaterial was obtained.

2.3. Apparatus and experiment procedures

The morphologies of the samples were observed by an S-4800 cold field scanning electron microscope (SEM, Hitachi, Japan) and a JEM-2100 transmission electron microscope (TEM, JEOL, Japan). UV–vis spectra were recorded on a Cary 50 UV-vis spectrophotometer (Varian, Australia). Infrared reflectance absorbance spectroscopy was conducted on 670 Fourier transform infrared spectrometer (Nicolet, USA).

Electrochemical measurements were performed on CHI-832 electrochemical analyzer (CHI, USA) with a three-electrode system comprising a gold wire as auxiliary electrode, a saturated calomel electrode as reference, against which all potentials were quoted, and the modified biosensor as working electrode. Cyclic voltammetric measurements were done at room temperature around 25 °C. Amperometric experiments were carried out in a stirred system with a working potential of −300 mV.

2.4. HRP immobilization and electrochemistry

HRP mixed with the PEDOT-PSS/Au colloid in PBS, with the final enzymatic concentration of 6.0 mg/mL, was prepared for further immobilization. The glass carbon electrode (GCE) is polished with 0.05 μm alumina and ultrasonic, and then dried. After that, the GCE is modified by dropping 5 μL of the prepared HRP/PEDOT-PSS/Au mixture onto the surface and dried in the air at room temperature. The prepared biosensor is reserved at room temperature during the whole experiment procedure.

3. Results and discussions

3.1. Characterization of PEDOT-PSS/Au nanocomposite

In this system, the PEDOT-PSS/Au nanocomposite was synthesized by chemical polymerization using $AuCl_3{\cdot}4H_2O$ as oxidant and PSS as dopant and cosolvent. As a cosolvent and water-soluble polyelectrolytes, PSS can improve the solubility of EDOT [25] in aqueous media. With the slowly addition of $AuCl_3{\cdot}4H_2O$, the initially colorless EDOT/PSS solution changed to green, then to grey, and finally to dark purple. The resulting dark purple solution indicates the formation of soluble PEDOT/Au nanomaterial due to the chemical polymerization of EDOT and reduction of Au^{3+}.

The morphology and size distribution of the nanomaterial is characterized by SEM and TEM. The conducting nanocomposite shows a fibrous structure and has a diameter of about 100 nm (Fig. 1a). The TEM clearly indicates that Au nanoparticles with a diameter of 3–5 nm were embedded into the framework of PEDOT-PSS (Fig. 1b). During the chemical polymerization process, the Au^{3+} could be well distributed along the polymer chains and the networks around Au^{3+} limited particle aggregation, therefore, the AuNPs in the films were dispersed uniformly throughout the films with small size. According to the EDS data (Fig. 1a inset), we can find that the materials containing Au, S and C elements, which suggests that PEDOT-PSS/Au nanomaterial has been successfully prepared.

The stability of PEDOT-PSS/Au nanomaterial in aqueous solution was further investigated, which is shown in Fig. 2. As a control experiment, while $AuCl_3{\cdot}4H_2O$ was added into EDOT solution without PSS, only blue sediments were obtained and precipitated within 120 min, indicating the formation of insoluble PEDOT materials (Fig. 2(a–d)). However, the PEDOT-PSS/Au nanocomposite is well-dispersed in aqueous solution and remains homogeneous in the whole experiment, even for 12 months (Fig. 2e) at room temperature, which indicates the encapsulation of AuNPs does not change the aqueous compatibility of PEDOT-PSS.

The UV–vis spectra further demonstrates the formation of PEDOT-PSS/Au nanomaterial (Fig. 3A(a)). After 20 min reaction, a broad absorption starting from 700 nm was observed, indicating the formation of PEDOT [26]. 110 min later, a weak peak at 523 nm was obtained, suggesting the formation of AuNPs [24]. A strong peak at 523 nm was observed when the reaction proceeding for 12 h, implying more AuNPs was generated.

3.2. HRP immobilization and characteristics

The UV–vis spectroscopy was used to investigate the immobilization of enzyme in PEDOT-PSS/Au nanomaterial. The peak located at 523 nm (Fig. 3A(a)) implies the formation of AuNPs [24]. After HRP immobilization, a new absorption peak located at 403 nm

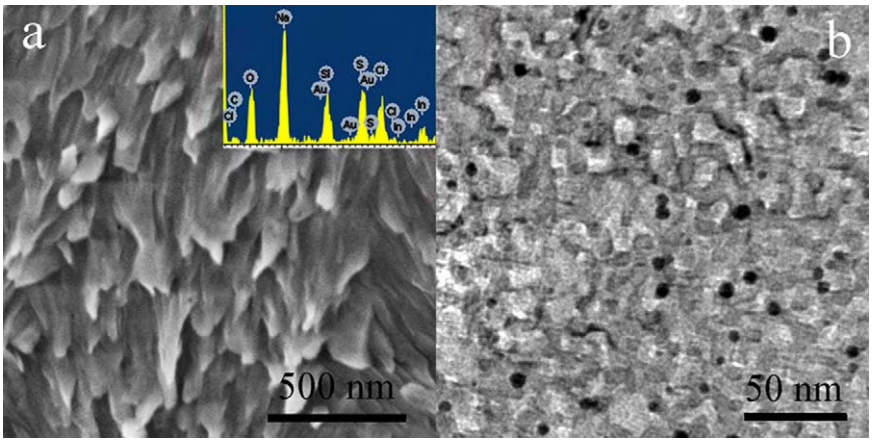

Fig. 1. SEM (a), TEM (b) and EDS (insert of (a)) images of PEDOT-PSS/Au nanocomposite.

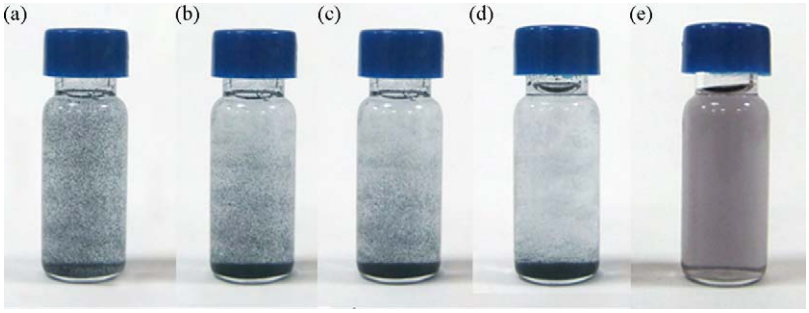

Fig. 2. Digital photographs of the PEDOT prepared without PSS (a–d) dispersed in PBS after 0 min (a), 10 min (b), 30 min (c), and 120 min (d). (e) The PEDOT-PSS/Au nanocomposite dispersed in PBS for 12 months.

is observed (Fig. 3A(b)), which is the characteristic signal of iron heme soret absorption. The location of the Soret absorption band of HRP in PEDOT-PSS/Au matrix is very close to that of in solution, and a difference of only 3 nm is observed. It suggests that the conformation of HRP is well remained [27]. Moreover, the characteristic absorptions of AuNPs and PEDOT is also be observed (Fig. 3A(b)).

FT-IR has been conducted in order to study the property of PEDOT-PSS/Au nanocomposite, and evaluate the bioactivity of the enzymes encapsulated into PEDOT-PSS/Au nanomaterial (Fig. 3B). In Fig. 3B(a), the peaks at 1647 and 1607 cm^{-1} are due to the stretching of the benzene in PSS, which is applied as a cosolvent and dopant. The peaks around 1520 cm^{-1} assign to the stretching of C=C in the thiophene ring. The peaks at 1041 and 1189 cm^{-1} in Fig. 3B are corresponding to the symmetric and asymmetric streching of S=O, and the bands from 600 to 850 cm^{-1} is due to the fingerprint absorption of PEDOT. These data demonstrate that the existence of PEDOT:PSS [28]. After the immobilization of HRP, the new peak at 1545 cm^{-1} is attributed to the vibration of amide II of HRP [29], indicating the plane bending of –N–H and stretching vibration of C–N in the peptide groups [30]. Both the sort band in UV–vis and vibration of amide II in FT-IR spectrograms demonstrate the successful encapsulation of HRP.

3.3. Direct electrochemistry of HRP and biosensing

Fig. 4A shows the cyclic voltammograms of PEDOT-PSS/Au, HRP/PEDOT-PSS/Au modified GCE in PBS (pH 7.2), and the electrochemical responses to hydrogen peroxide (H_2O_2). As for PEDOT-PSS/Au modified GCE, there is no evident peak observed at the electrochemical window (Fig. 4A(a)). However, a pair of redox peaks, located at −155 and −323 mV, appear at HRP/PEDOT-PSS/Au modified GCE, which results from the direct electron transfer between HRP and the underlying electrode (Fig. 4A(b)). The formal potential ($E^0 = (E_{ox} + E_{re})/2$) of the heme $Fe^{III/II}$ couple was −239 mV in 0.1 M pH 7.0 PBS, which suggests that most molecules preserved their native structure after being entrapped in the nanocomposite

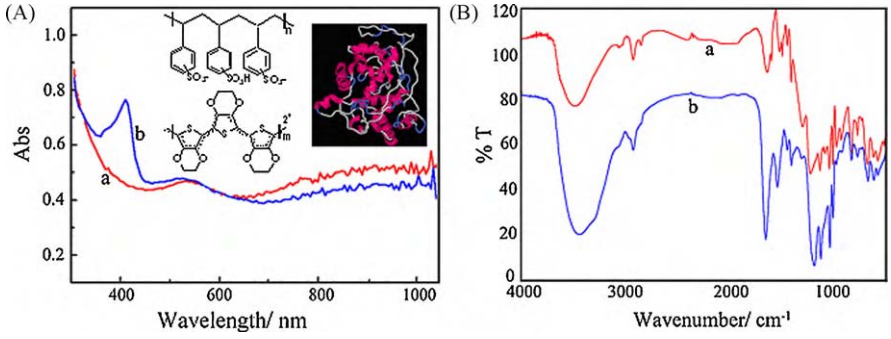

Fig. 3. UV–vis (A) and FT-IR (B) spectra of the PEDOT-PSS/Au nanocomposite before (a) and after HRP immobilized (b). Inset of (A) is the structure of PEDOT:PSS and HRP.

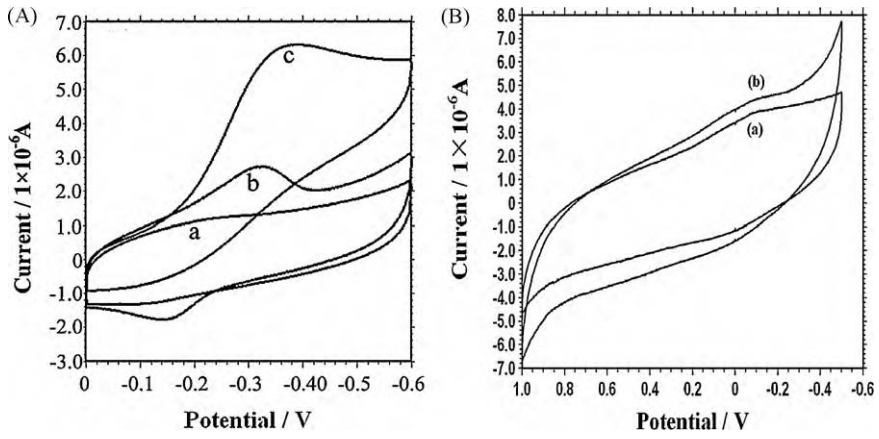

Fig. 4. (A) Cyclic voltammograms of the PEDOT-PSS/Au (a), HRP/PEDOT-PSS/Au in PBS without (b) and in presence of 0.8 mM H_2O_2 (c) at 100 mV/s. (B) Cyclic voltammograms of the PEDOT-PSS in PBS (A) and in the presence of 0.8 mM H_2O_2 (b).

[31]. The peak-to-peak separation is 168 mV, indicating a relative fast electron transfer process in this system. According to the theory of Laviron [32], the electron transfer rates k_s can be calculated by Eq. (1)

$$k_s = \frac{mnFv}{RT} \quad (1)$$

where m is a parameter related to the peak-to-peak separation, F is the Faraday's constant, R is the gas constant, T is the temperature, and n is the number of electron transfers. While the peak-to-peak separation is less than 200 mV, in this system, k_s turns out to be 0.47 s^{-1}. In order to investigation the function of Au nanoparticles in this system, a control experiment has been done. Without Au nanoparticles and HRP, no obvious catalytic current can be observed while H_2O_2 is added, which suggests that Au may act as an electron promoter in this system (Fig. 4B).

The effects of scan rates and pH on the electrochemical behaviors of HRP/PEDOT-PSS/Au modified GCE were also investigated. With the increasing scan rate from 0.01 to 0.5 V s^{-1}, the reduction and oxidation peak currents exhibit a linear relationship with the scan rate, indicating a surface-controlled electrochemical process [31]. While the solution pH varied from 5.0 to 10.0, the E^0 shifts negatively and has a linear relationship with pH with a slop of −50.8 mV/pH. It is close to the theoretical value of −58.5 mV/pH for a reversible, one-proton coupled one-electron reaction process at room temperature [33].

Effects of working potentials on the electrochemical responses are also investigated (Fig. 5) by successively addition of H_2O_2. It is observed that the reduction current at HRP/PEDOT-PSS/Au based biosensor with working potential of −300 mV is about two times than that operating in 0 mV. While conducting the experiment at more negative working potential, the increase of reduction currents is not obvious and the background currents are also increased. Therefore, the potential of −300 mV is selected as the optimized working potential.

Fig. 6 shows the amperometric responses of the biosensor with different concentrations of H_2O_2 from 0.2 to 100 μM. The reduction currents are linear within the concentration range from 2.0×10^{-7} to 3.8×10^{-4} M. The linear regression equation was i (μA) = 0.063c (μM) + 0.36 with a correlation coefficient of 0.99. The detection limit is 1.0×10^{-7} M (signal/noise = 3). When the concentration of H_2O_2 is higher than 1.0 mM, a plateau is obtained, which shows a characteristic reflection to the Michaelis–Menten kinetic mechanism. The apparent Michaelis–Menten constant K_m^{app} is an indication of both the enzymatic affinity and the enzyme-substrate kinetic constants, which can be obtained from Lineweaver–Burk

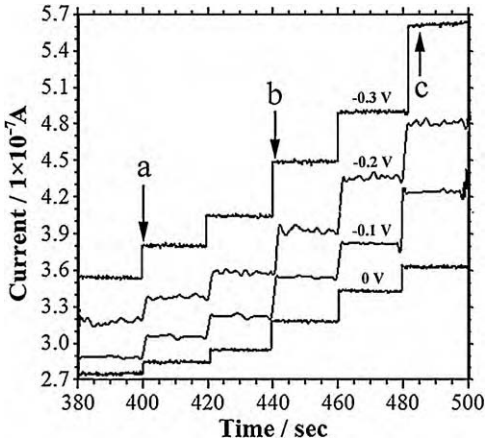

Fig. 5. Effects of working potential on the amperometric response of the HRP/PEDOT-PSS/Au based biosensor for 5.0 μM H_2O_2 (a), 10.0 μM H_2O_2 (b), and 20.0 μM H_2O_2 (c) at 100 mV/s.

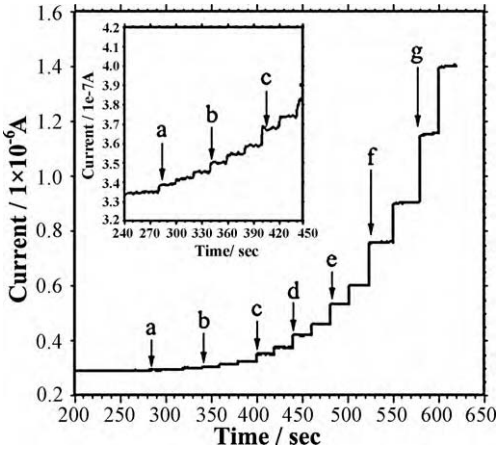

Fig. 6. Amperometric responses of the HRP/PEDOT-PSS/Au based biosensor for different concentrations of H_2O_2 in PBS (pH 7.2). (a–g: 0.2, 0.5, 1.0, 2.0, 10, 50, and 100 μM H_2O_2). Inset of figure is the enlargement of i–t responses of this biosensor for 0.2, 0.5, and 1.0 μM H_2O_2.

equation [32]:

$$\frac{1}{I_{ss}} = \frac{1}{I_{max}} + \frac{K_m^{app}}{I_{max} \cdot c} \quad (2)$$

Table 1
Real samples tested by the biosensor via standard addition method.

$C_{Original}$ (μM)	C_{Added} (μM)	C_{Found} (μM)	Recovery (%)
5.00	2.00	6.83	96.60
40.00	20.00	59.30	98.30
150.00	50.00	203.75	102.50

On the equation, I_{ss} is the steady-state current after the addition of substrate, c is the concentration of the substrate and I_{max} is the maximum current measured on saturated substrate condition. K_m^{app} is the reflection of the affinity of an enzyme for its substrate. A low K_m^{app} value indicates strong substrate binding. In this system, the K_m^{app} of HRP/PEDOT-PSS/Au electrode is found to be 0.78 mM, which is lower that of 11 mM for HRP in solution [34]. In addition, this value was smaller than those of 2.33 mM for HRP immobilized in chitosan/carbon microsphere microbiocomposites [35], 2.3 mM for HRP immobilized on a colloid/cysteamine modified gold electrode [36], and 5.5 mM for HRP immobilized in polymer [37]. It proves that the biosensor has good biocompatibility and HRP in the biosensor remains high activity.

The stability of the HRP immobilized into PEDOT-PSS/Au nanocomposites was evaluated via the continuous cyclic scans. After 100 scans, no obvious changes of the redox currents was observed, indicating few leaching of HRP. The stability of this biosensor was further investigated by amperometric detection of 50 μM H_2O_2. The amperometric response of the biosensor still retains over 90% of its initial sensitivity to the reduction of H_2O_2, even the HRP/PEDOT-PSS/Au electrode was stored in refrigerator at 4 °C in pH 7.2 PBS for 3 weeks. It indicates that the stability of this biosensor is very well. However, when the concentration of H_2O_2 is higher than 5.0 mM, the electrochemical response of the biosensor decreases rapidly. It is because that the normal catalytic cycle for HRP could be inhibited at high H_2O_2 concentrations [38]. The inactivation routes include two pathways. The first is the irreversible conversion of HRP-I (the oxidized form of the enzyme containing an oxyferryl group (Fe^{IV}=O) and a π-cation radical in the porphyrin ring) into a verdohaemoprotein (P670), a dead end in the catalytic cycle [39]. The second is the formation of oxyperoxidase (commonly known as HRP-III), leading to the inactivation of enzyme [40]. Thus, high concentration of H_2O_2 should be avoided in order to maintain the bioactivity and catalytic activity of HRP over a longer period.

3.4. Real sample analysis

With the purpose to verify the applicability of the proposed biosensor for real sample analysis, three water samples with different concentrations of H_2O_2 were measured by standard addition method, and the recovery rate of the real samples is also obtained (Table 1). From Table 1, we can find the recovery rate is over the range of 96.6–102.5%, which suggests the biosensor can be used for real sample analysis.

4. Conclusion

With a highly soluble, fibroid PEDOT-PSS/Au nanocomposite, HRP has been immobilized with high bioactivity. The direct electron transfer of immobilized enzymes and the excellent electrochemical responses of HRP/PEDOT-PSS/Au toward H_2O_2 suggest that the soluble PEDOT-PSS/Au matrix can provide a biocompatible platform for enzyme immobilization and biosensing.

Acknowledgments

This work was supported by the National Natural Science Foundation of China (No. 20875031), Shanghai Rising-Star Program (No. 09QH1400800), New Century Excellent Talents in University (No. NCET-09-0357) and Shanghai Municipal Education Commission (No. 08ZZ25).

References

[1] A.G. Bayer, Eur. Patent, 339 340 (1988).
[2] L.B. Groenendaal, F. Jonas, D. Freitag, H. Pielartzik, J.R. Reynolds, Adv. Mater. 12 (2000) 481.
[3] F. Jonas, J.T. Morrison, Synth. Met. 85 (1997) 1397.
[4] J.A. Lim, S.H. Park, J.H. Baek, Y.D. Ko, H.S. Lee, K. Cho, J.Y. Lee, D.R. Lee, J.H. Cho, Appl. Phys. Lett. 95 (2009) 233509.
[5] P. Ravirajan, S.A. Haque, J.R. Durrant, D.D.C. Bradley, J. Nelson, Adv. Funct. Mater. 15 (2005) 609.
[6] S.I. Cho, D.H. Choi, S.H. Kim, S.B. Lee, Chem. Mater. 17 (2005) 4564.
[7] B. Zhang, W. Li, J. Yang, Y. Fu, Z. Xie, S. Zhang, L. Wang, J. Phys. Chem. C 113 (2009) 7898.
[8] S.M. Richardson-Burns, J.L. Hendricks, B. Foster, L.K. Povlich, D.H. Kim, D.C. Martin, Biomaterials 28 (2007) 1539.
[9] J. Isaksson, P. Kjall, D. Nilsson, N.D. Robinson, M. Berggren, A. Richter-Dahlfors, Nat. Mater. 6 (2007) 673.
[10] M. Onoda, Y. Abe, K. Tada, Thin Solid Films 518 (2009) 743.
[11] M. Asplund, E. Thaning, J. Lundberg, A.C. Sandberg-Nordqvist, B. Kostyszyn, O. Inganas, H. von Holst, Biomed. Mater. 4 (2009) 45009.
[12] S.C. Luo, E.M. Ali, N.C. Tansil, H.H. Yu, S. Gao, E.A.B. Kantchev, J.Y. Ying, Langmuir 24 (2008) 8071.
[13] D.F. Li, H.J. Wang, J.X. Fu, W. Wang, X.S. Jia, J.Y. Wang, J. Phys. Chem. B 112 (2008) 16290.
[14] A. Roucoux, J. Schulz, H. Patin, Chem. Rev. 102 (2002) 3757.
[15] M.S. Chen, D.W. Goodman, Science 306 (2004) 252.
[16] M. Menon, D. Srivastava, Phys. Rev. Lett. 79 (1997) 4453.
[17] E. Katz, I. Willner, Angew. Chem. Int. Ed. 43 (2004) 6042.
[18] J.S. Lee, M.S. Han, C.A. Mirkin, Angew. Chem. Int. Ed. 46 (2007) 4093.
[19] W.P. Hall, O. Lyandres, N.C. Shah, J. Zhao, R.P. Van Duyne, Nat. Mater. 7 (2008) 442.
[20] K.M. Manesh, P. Santhosh, A. Gopalan, K.P. Lee, Talanta 75 (2008) 1307.
[21] J. Mathiyarasu, S. Senthilkumar, K.L.N. Phani, V. Yegnaraman, Mater. Lett. 62 (2008) 571.
[22] A.N. Shipway, M. Lahav, I. Willner, Adv. Mater. 12 (2000) 993.
[23] N. Nath, A. Chilkoti, Anal. Chem. 76 (2004) 5370.
[24] S.S. Kumar, C.S. Kumar, J. Mathiyarasu, K.L. Phani, Langmuir 23 (2007) 3401–3408.
[25] E. Tamburri, S. Orlanducci, F. Toschi, M.L. Terranova, D. Passeri, Synth. Met. 159 (2009) 406.
[26] W.C. Chen, C.L. Liu, C.T. Yen, F.C. Tsai, C.J. Tonzola, N. Olson, S.A. Jenekhe, Macromolecules 3 (2004) 5959.
[27] X.B. Lu, Q. Zhang, L. Zhang, J.H. Li, Electrochem. Commun. 8 (2006) 874.
[28] C.A. Cutler, M. Bouguettaya, T.S. Kang, J.R. Reynolds, Macromolecules 38 (2005) 3068.
[29] J.K. Kauppinen, D.J. Moffatt, H.H. Mantsch, D.G. Cameron, Appl. Spectr. 35 (1981) 271.
[30] J.W. Hare, E.I. Solomon, H.B. Gray, J. Am Chem. Soc. 98 (1976) 3205.
[31] S.Z. Zong, Y. Cao, Y.M. Zhou, H.X. Ju, Langmuir 22 (2006) 8915.
[32] E. Laviron, J. Electroanal. Chem. 101 (1979) 19.
[33] X.H. Kang, J. Wang, Z.W. Tang, H. Wu, Y.H. Lin, Talanta 78 (2009) 120.
[34] S.Q. Liu, H.X. Ju, Anal. Biochem. 307 (2002) 110.
[35] X. Chen, C.C. Li, Y.L. Liu, Z.F. Du, S.J. Xu, L.M. Li, M. Zhang, T.H. Wang, Talanta 77 (2008) 37.
[36] Y. Xiao, H.X. Ju, H.Y. Chen, Anal. Biochem. 278 (2000) 22.
[37] T. Ferri, A. Poscia, R. Santucci, Bioelectrochem. Bioenergy 45 (1998) 221.
[38] J.J. Calvente, A. Narváez, E. Domínguez, R. Andreu, J. Phys. Chem. B 107 (2003) 6629.
[39] J. Hernadez-Ruiz, M.B. Arnao, A.N.P. Hiner, F. Garcia-Canovas, M. Acosta, Biochem. J. 354 (2001) 107.
[40] M. Dequaire, B. Limoges, J. Moiroux, J.M. Savéant, J. Am. Chem. Soc. 124 (2002) 240.